EJN
European Journal of Neuroscience

European Journal of Neuroscience, Vol. 27, pp. 2515–2528, 2008 doi:10.1111/j.1460-9568.2008.06234.x

Postnatal changes in somatic γ-aminobutyric acid signalling in the rat hippocampus

Roman Tyzio,[1] Marat Minlebaev,[1] Sylvain Rheims,[1] Anton Ivanov,[1] Isabelle Jorquera,[1] Gregory L. Holmes,[2] Yuri Zilberter,[1] Yehezkiel Ben-Ari[1] and Rustem Khazipov[1]
[1]Inmed/Inserm U901, Université de la Méditerranée, 163, Avenue de Luminy, 13273 Marseille, France
[2]Department of Neurology, Neuroscience Center at Dartmouth, Dartmouth Medical School, Lebanon, NH, USA

Keywords: development, membrane potential, patch-clamp, single channels

Abstract

During postnatal development of the rat hippocampus, γ-aminobutyric acid (GABA) switches its action on CA3 pyramidal cells from excitatory to inhibitory. To characterize the underlying changes in the GABA reversal potential, we used somatic cell-attached recordings of GABA(A) and *N*-methyl-D-aspartate channels to monitor the GABA driving force and resting membrane potential, respectively. We found that the GABA driving force is strongly depolarizing during the first postnatal week. The strength of this depolarization rapidly declines with age, although GABA remains slightly depolarizing, by a few millivolts, even in adult neurons. Reduction in the depolarizing GABA driving force was due to a progressive negative shift of the reversal potential of GABA currents. Similar postnatal changes in GABA signalling were also observed using the superfused hippocampus preparation *in vivo*, and in the hippocampal interneurons *in vitro*. We also found that in adult pyramidal cells, somatic GABA reversal potential is maintained at a slightly depolarizing level by bicarbonate conductance, chloride-extrusion and chloride-loading systems. Thus, the postnatal excitatory-to-inhibitory switch in somatic GABA signalling is associated with a negative shift of the GABA reversal potential but without a hyperpolarizing switch in the polarity of GABA responses. These results also suggest that in adult CA3 pyramidal cells, somatic GABAergic inhibition takes place essentially through shunting rather than hyperpolarization. Apparent hyperpolarizing GABA responses previously reported in the soma of CA3 pyramidal cells are probably due to cell depolarization during intracellular or whole-cell recordings.

Introduction

γ-Aminobutyric acid (GABA) is the main inhibitory neurotransmitter in the adult brain (Farrant & Kaila, 2007). However, early in development, GABA, acting via chloride-permeable GABA(A) channels, exerts an excitatory action due to elevated $[Cl^-]_i$ in the immature neurons (Cherubini *et al.*, 1991; Ben-Ari *et al.*, 1997; Ben Ari, 2002; Owens & Kriegstein, 2002; Ben Ari *et al.*, 2007). Maturation of GABAergic signalling in CA3 pyramidal cells of the rat hippocampus is characterized by two excitatory-to-inhibitory (E–I) switches in GABA's action. The first near-term E–I switch is transient and is mediated by the action of maternal oxytocin (Tyzio *et al.*, 2006). The second developmental E–I switch is permanent, occurring during the second postnatal week (Khazipov *et al.*, 2004; Tyzio *et al.*, 2007); and is due to progressive changes in the expression of the chloride membrane transporters (Rivera *et al.*, 1999; Ganguly *et al.*, 2001; Payne *et al.*, 2003; Yamada *et al.*, 2004; Dzhala *et al.*, 2005).

Both the near-term and postnatal E–I switches in GABA action on CA3 pyramidal cells are thought to be due to the switch in the polarity of GABAergic responses from depolarizing to hyperpolarizing (Obata *et al.*, 1978; Mueller *et al.*, 1984; Ben-Ari *et al.*, 1989; Swann *et al.*, 1989; Luhmann & Prince, 1991; Psarropoulou & Descombes, 1999; Rivera *et al.*, 1999; Banke & McBain, 2006; Tyzio *et al.*, 2006). The action of GABA depends on the direction of the transmembrane current elicited by GABA, its driving force (DF_{GABA}) being the difference between the GABA(A) reversal potential (E_{GABA}) and resting membrane potential (E_m). Using noninvasive cell-attached recordings of single GABA(A) and *N*-methyl-D-aspartate (NMDA) channels from CA3 pyramidal cells to monitor DF_{GABA} and E_m, it has been shown that the near-term E–I switch in the GABA action is associated with a change in the polarity of DF_{GABA} from depolarizing to hyperpolarizing due to a negative shift of E_{GABA} (Tyzio *et al.*, 2006). Studies using sharp electrodes and gramicidin-perforated patch recordings have also suggested that the postnatal E–I switch is associated with a change in the polarity of DF_{GABA} from depolarizing to hyperpolarizing (Mueller *et al.*, 1984; Ben-Ari *et al.*, 1989; Swann *et al.*, 1989; Psarropoulou & Descombes, 1999; Rivera *et al.*, 1999; Banke & McBain, 2006). However, intracellular and gramicidin-perforated patch recordings may introduce several sources of error in the estimation of GABA actions, including neuronal depolarization and modification of $[Cl^-]_i$, both of which may affect measurements in small immature cells (Ben-Ari *et al.*, 1989; Barry & Lynch, 1991; Staley *et al.*, 1992; Tyzio *et al.*, 2003). Therefore, it remains unclear whether the postnatal E–I switch in the GABA action is associated with a depolarizing-to-hyperpolarizing switch in GABA responses.

Maturation of GABA signalling in specific cell compartments is yet another poorly understood phenomenon. A considerable amount of

Correspondence: R. Khazipov, as above.
E-mail: khazipov@inmed.univ-mrs.fr

Received 19 January 2007, revised 26 March 2008, accepted 31 March 2008

evidence indicates that E_{GABA} may differ in various parts of the cell and that it even displays synapse-specific plasticity (Woodin *et al.*, 2003; Fiumelli & Woodin, 2007). Several gradients of E_{GABA} have been described, including somatodendritic and axon initial segment–somatic gradients (Hara *et al.*, 1992; Szabadics *et al.*, 2006; Khirug *et al.*, 2008; Romo-Parra *et al.*, 2008) [but see also Gulledge & Stuart (2003)]. However, little is known about how E_{GABA} changes with development in various cell compartments. Recent work using extracellular field potential and intracellular recordings suggested that, during development, E_{GABA} shifts from depolarizing to hyperpolarizing values earlier in the soma than in dendrites (Romo-Parra *et al.*, 2008). This may reflect developmental NKCC1 migration from the soma to dendrites (Marty *et al.*, 2002). On the other hand, an opposite relationship between E_{GABA} in the soma and dendrites (more hyperpolarizing in dendrites than in the soma) has been suggested in adult neurons (Khirug *et al.*, 2008).

In the present study, we examined postnatal changes of E_{GABA} in the somatic compartment of hippocampal CA3 pyramidal cells using cell-attached recordings of single GABA and NMDA channels to monitor the GABA driving force and resting membrane potential, respectively. An important advantage of this noninvasive technique is that it permits punctual measurements of E_{GABA} in approximately 1 μm^2 of recorded patch from the cell membrane. We found that during postnatal development, there is a progressive negative shift in E_{GABA}. However, in contrast to the near-term switch, the postnatal E–I switch was not associated with a change in the polarity of the GABAergic responses, which remained slightly depolarizing even in adult CA3 pyramidal cells. These results also suggest that in adult CA3 pyramidal cells, which have been widely considered to be prototypes of neurons with classic hyperpolarizing inhibitory postsynaptic potentials, somatic GABAergic inhibition is essentially shunting, not hyperpolarizing, as has been previously suggested for some other types of neurons (Eccles *et al.*, 1961; Barrett & Crill, 1974; Kennedy *et al.*, 1974; Misgeld *et al.*, 1986; Edwards, 1990; Staley & Mody, 1992; Kaila *et al.*, 1993; Zhang & Jackson, 1993; Golding & Oertel, 1996; Cattaert & El Manira, 1999; Rudomin & Schmidt, 1999; Lu & Trussell, 2001; Martina *et al.*, 2001; Monsivais & Rubel, 2001; Bartos *et al.*, 2002; Chavas & Marty, 2003; Gulledge & Stuart, 2003; Banke & McBain, 2006; Vida *et al.*, 2006). Pyramidal neurons recorded in the superfused hippocampal preparation from anaesthetized rats *in vivo* had a similar paradigm. Likewise, during the postnatal period, somatic GABA action shifted from depolarizing to slightly hyperpolarizing in the majority of hippocampal interneurons.

Materials and methods

Hippocampal slices

Hippocampal slices were prepared from Wistar rats. All animal use protocols conformed to the national guidelines on the use of laboratory animals and were approved by the Animal Care and Use Committee of INSERM. Animals were anaesthetized with chloral hydrate (350 mg/kg, intraperitoneally) and decapitated. The brain was removed, and transverse slices (350–500 μm) were cut from the middle part of the hippocampus using a Vibratome (VT 1000E; Leica, Nussloch, Germany). Slices were kept in oxygenated (95% O_2/5% CO_2) artificial cerebrospinal fluid (ACSF) composed of NaCl 126 mM, KCl 3.5 mM, $CaCl_2$ 2.0 mM, $MgCl_2$ 1.3 mM, $NaHCO_3$ 25 mM, NaH_2PO_4 1.2 mM and glucose 11 mM (pH 7.4) at room temperature (20–22 °C) for at least 1 h before use. For recordings, slices were placed into a conventional, fully submerged, chamber superfused with ACSF (30–32 °C) at a rate of 2–3 ml/min.

Cell-attached recordings of GABA and NMDA channels

Patch-clamp recordings from visually identified CA3 pyramidal cells and interneurons in a cell-attached configuration were performed using an EPC-10 double amplifier (HEKA Elektronik Dr Schulze GmbH, Lambrecht/Pfalz, Germany) or Axopatch 200B amplifier (Axon Instruments, Union City, CA, USA). For recordings of single GABA(A) channels, patch pipette solution containing NaCl 120 mM, tetraethylammonium–Cl 20 mM, KCl 5 mM, 4-aminopyridine 5 mM, $CaCl_2$ 0.1 mM, $MgCl_2$ 10 mM, glucose 10 mM and Hepes–NaOH 10 mM buffered to pH 7.2–7.3, and GABA (1–5 μM), was added on the day of the experiment from a 1 mM frozen stock solution. Because the composition of the solution for cell-attached recordings differs from that of ACSF, this may introduce a systematic error into the estimation of DF_{GABA}. This error was estimated experimentally in two series of experiments. In the first series, we determined the reversal potential of the currents via GABA(A) channels in outside-out patches. In these experiments 2 mM MgATP and 5 mM EGTA were added to the pipette solution to prevent rundown of GABA currents. Brief pressure application of isoguvacine (100 μM, 100 ms, 2–8 psi) to the outside-out or nucleated patches evoked GABA(A) receptor-mediated currents that were completely suppressed by the GABA(A) receptor antagonist bicuculline (20 μM; $n = 2$, not shown). Study of the current–voltage relationships revealed that these responses have a mean conductance of 1.4 ± 0.4 nS and a reversal potential of +2.1 ± 0.4 mV ($n = 7$ outside-out and $n = 1$ nucleated patch; Fig. 1).

In the second series of experiments, we measured DF_{GABA} using pipette solution containing ACSF and GABA (2 μM) in 1-month-old rats. To maintain pH at a physiological level, pipette ACSF was continuously oxygenated with 95% O_2/5% CO_2 via a patch pipette holder. The value of DF_{GABA} with ACSF-based pipette solution was 4.0 ± 0.6 mV ($n = 9$), as compared to 5.4 ± 1.3 mV ($n = 4$) obtained using the principal pipette solution for GABA channel recordings. The difference of 1.6 mV was close to that obtained using outside-out patches (2.1 mV). Because outside-out patch recordings give highly precise estimates of the reversal potential (Fig. 1), all values of DF_{GABA} obtained with the principal solution for cell-attached GABA channel recordings were corrected for 2.1 mV obtained using outside-out recordings.

Membrane potential was estimated using cell-attached recordings of single NMDA channels as described previously (Leinekugel *et al.*, 1997; Tyzio *et al.*, 2003). For recordings of single NMDA channels, pipette solution contained nominally Mg^{2+}-free ACSF with NMDA (10 μM), glycine (1 μM) and strychnine (1 μM). This approach has a substantial advantage in comparison to whole-cell recordings, because it does not cause cell depolarization due to introduction of leak conductance – the error that is particularly important in small immature neurons with high membrane resistance (Tyzio *et al.*, 2003). To estimate the reliability of this technique for E_m measurements, we performed the experiment illustrated in Fig. 2, using dissociated cultures of rat hippocampus at 16–21 days *in vitro*. We first estimated E_m in the intact cell using cell-attached recordings of NMDA channels, which gave a value of −81 ± 3 mV [$n = 3$ for dual recordings (Fig. 2A); −76 ± 2 mV; $n = 8$ for single cell-attached recordings]. Keeping cell-attached recordings, the cell was patched with a second pipette and recorded in whole-cell mode (Fig. 2B). Under these recording conditions, E_m deduced from cell-attached recordings of NMDA channels shifted to a more depolarized value of −54 ± 4 mV ($n = 3$), which was close to the E_m value measured directly in whole-cell recordings (−56 ± 3 mV; $n = 72$), and the difference between these two values was within ±3 mV [0.9 ± 1.3 mV (mean ± SE); $n = 3$]. These results support our previous conclusion

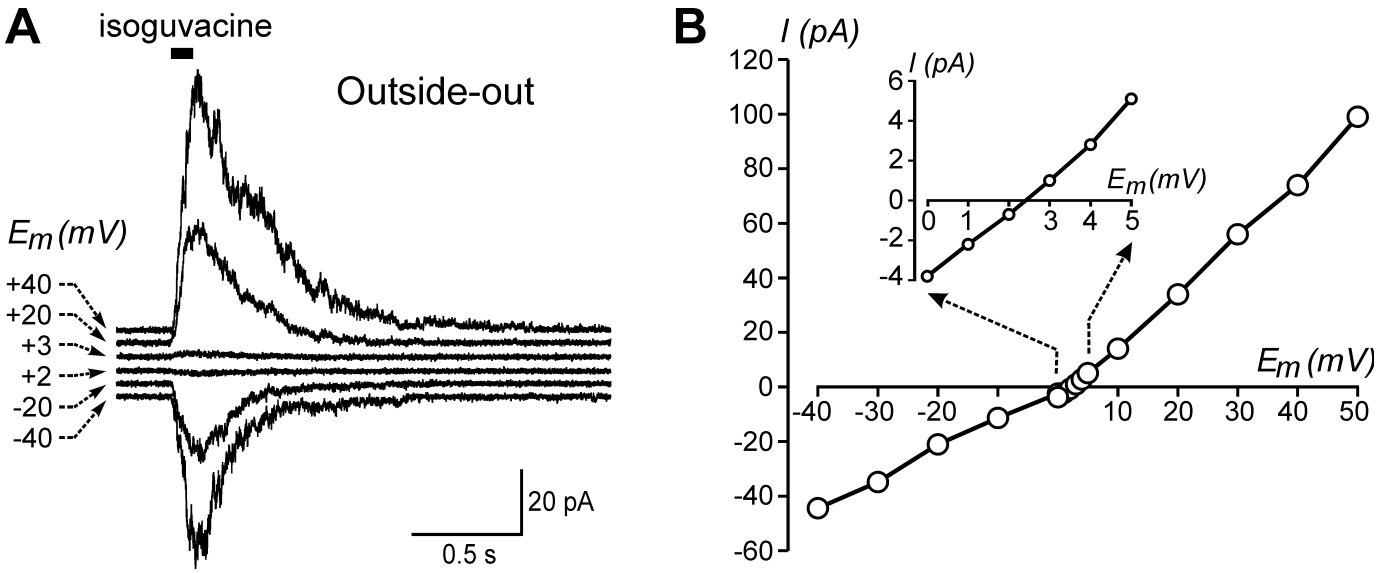

FIG. 1. Estimations of the correction factor for the solution for cell-attached measurements of the γ-aminobutyric acid (GABA) driving force using outside-out patch recordings. (A) Outside-out recordings of the responses evoked by brief application of the GABA(A) receptor agonist isoguvacine (100 μM, 100 ms) at different holding potentials. The pipette was filled with a solution for cell-attached recordings of GABA channels; the external solution was artificial cerebrospinal fluid. (B) Corresponding *I–V* relationships of the GABA(A) receptor-mediated currents. Note the reversal potential near +2 mV.

that cell-attached recordings of NMDA channels provide a reliable estimate of E_m, and they raise further concern about neuronal depolarization introduced in whole-cell recordings.

In vivo *recordings*

Hippocampal recordings *in vivo* were performed using a superfused hippocampus preparation as described previously (Khazipov & Holmes, 2003). In brief, rats were anaesthetized with 1–2 g/kg urethane injected intraperitoneally. The skin and periosteum were removed from the skull, which was then covered with a layer of dental acrylic, except for an area ~5 mm in diameter above the hippocampus. The rat was positioned in the stereotaxic apparatus, and the skull was attached to the nose (nasal bones) and ear bars (occipital bone) with dental acrylic. A burr hole of diameter 5 mm was drilled in the skull above the hippocampus. The dura was cut and removed, and the neocortex above the hippocampus was removed by vacuum suction. The hippocampal surface was covered with 0.9% NaCl during the procedure to prevent it from drying. The perfusion chamber was prepared as described previously (Khazipov & Holmes, 2003; Minlebaev *et al.*, 2007), with some modifications. A 4-mm-long cylinder was cut from a plastic tube (inner diameter 3.5 mm; outer diameter 4.5 mm) and glued to stretched nylon mesh (pore diameter 120 μm) with cyanoacrylamide glue. The chamber was positioned at the hippocampal surface so that the mesh gently pressed onto the hippocampus. The chamber was then fixed to the skull with dental acrylic. Chlorided silver wire was placed into the perfusion chamber, and served as a ground electrode. During the recordings, rats were heated via a thermal pad (37 °C). The chamber was perfused with oxygenated ACSF at a rate of 2 ml/min. The temperature in the chamber was kept at 35–37 °C using an automatic temperature controller (TC-344B; Warner Instruments, Hamden, CT, USA). Patch-clamp recordings were performed from the pyramidal cell layer (depth 100–200 μm) using an Axopatch 200B amplifier (Axon Instruments), using a patching technique similar to that described *in vivo* (Leinekugel *et al.*, 2002; Khazipov & Holmes, 2003; Minlebaev *et al.*, 2007).

Recordings were digitized (10 kHz) online with Digidata 1200 or 1440 interface cards (Axon Instruments) and analysed offline with Axon package (Axon Instruments) and Origin (Microcal Software, Northampton, MA, USA) as described previously (Khazipov *et al.*, 1995; Tyzio *et al.*, 2003, 2006). Group measures are expressed as means ± SEM; error bars also indicate SEM. The statistical significance of differences was assessed with Student's *t*-test. The level of significance was set at $P < 0.05$.

Morphology

In the series of recordings from interneurons, all the recorded slices were processed for biocytin-filled neuron detection as described previously (Khazipov *et al.*, 2001). Whole-cell recordings of interneurons were performed using a solution composed of 115 mM potassium gluconate, 20 mM KCl, 4 mM MgATP, 10 mM sodium phosphocreatine, 0.3 mM NaGTP, 10 mM Hepes, and 0.5% biocytin, adjusted to pH 7.3 with NaOH. The slices were fixed overnight at room temperature in a solution containing 4% paraformaldehyde in 0.1 M phosphate-buffered saline (PBS; pH 7.4). After fixation, slices were rinsed in PBS, cryoprotected in sucrose for 16 h, and quickly frozen on dry ice. The detection of biocytin-filled neurons was performed on unsectioned slices. To neutralize an endogenous peroxidase, slices were pretreated for 30 min in 1% H_2O_2. After several rinses in 0.1 M PBS (pH 7.4), slices were incubated for 24 h at 4 °C in 1 : 100 avidin-biotinylated peroxidase complex diluted in PBS containing 0.3% Triton X-100. After 30 min rinses in PBS, slices were processed with 0.06% 3,3′-diaminobenzidine tetrahydrochloride (Sigma, St Louis, MO, USA) and 0.006% H_2O_2 diluted in PBS, rinsed, mounted on gelatin-coated slides, and coverslipped in an aqueous medium (Crystal/Mount; Biomeda, Foster City, CA, USA). Interneurons were morphologically identified on the basis of their dendritic and axonal arborizations.

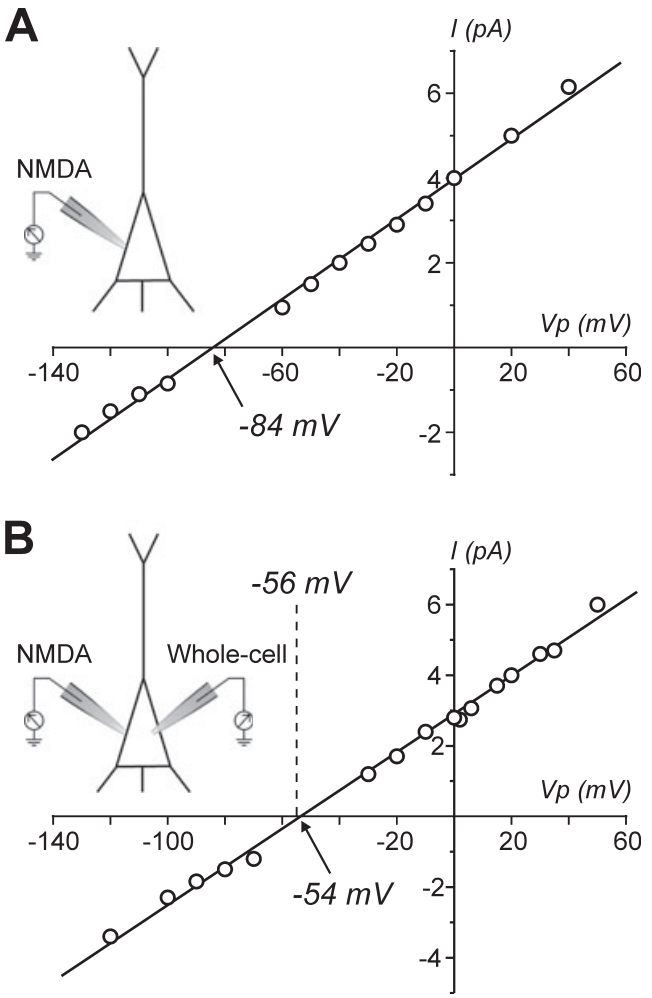

FIG. 2. Comparison of the membrane potentials measured using dual cell-attached recordings of *N*-methyl-D-aspartate (NMDA) channels and whole-cell recordings. (A) NMDA channels were recorded with a single patch pipette in cell-attached mode. *I–V* relationships of NMDA currents give an E_m estimate of −84 mV (arrow). (B) Dual whole-cell and cell-attached recordings from the same cell estimated E_m at −56 mV (dashed line) and −54 mV (arrow), respectively. Note that the whole-cell recordings cause strong neuronal depolarization. V_p, pipette potential.

Results

Postnatal changes of E_{GABA} *in the soma of CA3 pyramidal cells*

To characterize the postnatal changes in the GABA(A) driving force, we used cell-attached recordings of single GABA channels from the soma of CA3 pyramidal cells in the hippocampal slices from the rats aged from postnatal day (P)1 to P30 (n = 133 cells). This noninvasive single GABA channel recording technique has substantial advantages over other electrophysiological approaches to measure DF_{GABA}, because it affects neither E_{GABA} nor E_m (Serafini *et al.*, 1995; Tyzio *et al.*, 2006). In addition, this methodology is not compromised by space-clamp problems. Typical records of GABA channels from P1, P15 and P30 neurons at different pipette potentials (V_p) are shown in Fig. 3. Currents through GABA(A) channels displayed outward rectification: outwardly directed currents at negative values of V_p were larger than inwardly directed currents at positive values of V_p. The current–voltage relationships were best fitted with an exponential function. The tangent to the *I–V* curve at the reversal potential gave an estimate of the conductance of 16.9 ± 1.7 pS (mean ± EM; n = 133).

In cell-attached recordings, the driving force on ions across GABA(A) channels is $-DF_{GABA} - V_p$. Therefore, DF_{GABA} equals $-V_p$ at the reversal potential of the currents through GABA(A) channels. From the *I–V* curves for the currents through single GABA(A) channels, DF_{GABA} was inferred to be dependent on age. During the first postnatal week, DF_{GABA} was strongly positive, with a maximal value of 17.4 ± 3.4 mV at P1 (n = 6), and was highly variable. During the first two postnatal weeks, DF_{GABA} shifted progressively and negatively to reach 3.6 ± 1.0 mV at P15–P30 (n = 39; Fig. 4). The postnatal negative shift in DF_{GABA} was accompanied by reduction in the variation of DF_{GABA} values, evident as a reduction in the standard error in Fig. 4. Thus, noninvasive measurements of DF_{GABA} using cell-attached recordings of GABA channels indicate that during postnatal development, there is a progressive reduction in the amplitude of somatic depolarizing DF_{GABA} that remains slightly depolarizing even in adult neurons, and that somatic GABA responses do not switch polarity from depolarizing to hyperpolarizing with development.

The developmental changes in DF_{GABA} could be due either to a negative shift of E_{GABA} or to a depolarizing shift of E_m. Therefore, we also measured E_m, using single NMDA channels in cell-attached recordings as a voltage sensor (Leinekugel *et al.*, 1997; Tyzio *et al.*, 2003, 2006). Dual cell-attached recordings of GABA(A) and NMDA channels were performed in 43 CA3 pyramidal cells at P3, P9, P18, and P30. Typical simultaneous recordings of GABA(A) and NMDA channels from the soma of the same neuron are shown in Fig. 5A. That recordings were made from the same neuron was ensured by the presence of synchronous action potentials in cell-attached recordings and/or synchronous synaptic activity in subsequent whole-cell recordings (Fig. 5B and C). In keeping with previous results, the average E_m inferred from the *I–V* curves of the currents through NMDA channels was around −78 ± 2 mV, and did not significantly change during postnatal development (Tyzio *et al.*, 2003, 2006). Knowing DF_{GABA} and E_m, from the recordings of single GABA(A) and NMDA channels, respectively, we further calculated E_{GABA} ($E_{GABA} = DF_{GABA} + E_m$) for each neuron. We found that E_{GABA} shifted from a depolarizing value of −63.5 ± 1.4 mV at P3 to a slightly depolarizing value of −75.2 ± 0.9 mV at P18, without any significant change with further maturation (−75.3 ± 0.9 mV at P30; n = 5; Fig. 5D).

E_{GABA} *in interneurons*

Previous studies have shown that GABA signalling also undergoes developmental changes in the hippocampal interneurons, although the results are variable (Leinekugel *et al.*, 1995; Khazipov *et al.*, 1997; Verheugen *et al.*, 1999; Banke & McBain, 2006; Fu & van den Pol, 2007). We measured DF_{GABA}, E_m and E_{GABA} using cell-attached recordings in the soma of hippocampal interneurons in two age groups, P2–P4 and P21–P28. In this series of experiments, visually identified interneurons were first patched to record NMDA and GABA channels, and then filled with biocytine in whole-cell mode for further morphological identification. In the P2–P4 age group, 12 interneurons were recorded, and 11 of them were successfully labelled with biocytine and identified as interneurons with the soma located in the stratum radiatum (n = 2), stratum lucidum (n = 8) and stratum oriens (n = 1). E_m ranged from −65 to −87 mV (mean: −73 ± 2 mV), and DF_{GABA} was positive, ranging from 3 to 26 mV, except for one interneuron, which had a DF_{GABA} of −8 mV (mean for all cells,

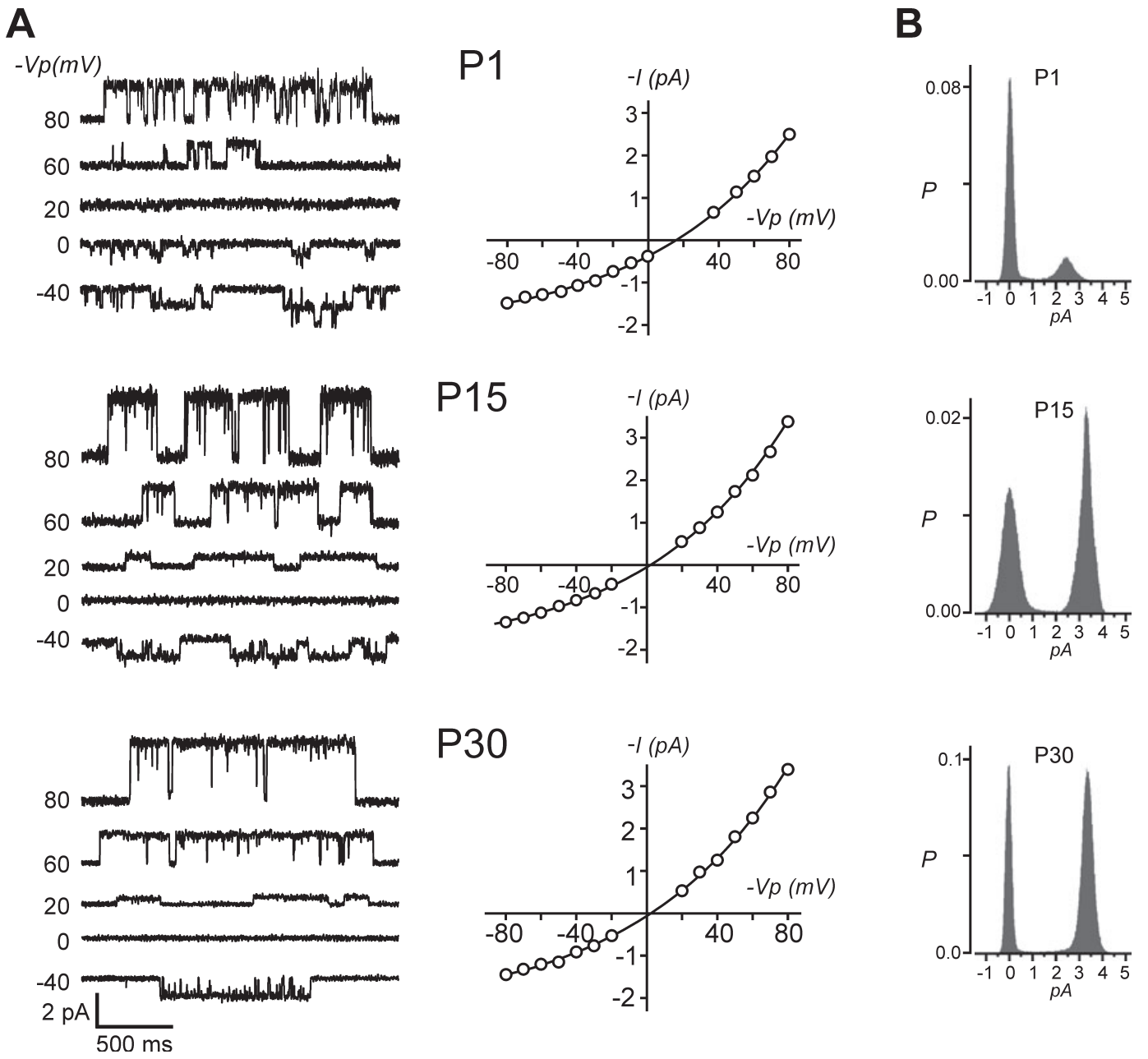

FIG. 3. Measurement of the γ-aminobutyric acid (GABA)(A) driving force in the soma of CA3 pyramidal cells using cell-attached recordings of single GABA(A) channels. (A) Cell-attached recordings of single GABA(A) channels with 1 μM GABA in a patch pipette at different pipette potentials (V_p) at postnatal day (P)1, P15 and P30. Traces are inverted because inwardly directed currents in cell-attached recordings correspond to inwardly directed currents through the membrane. On the right, Corresponding *I–V* relationships of the currents through single GABA channels. Each point is a mean amplitude of about 30 openings at a given V_p. The reversal potential that corresponds to the GABA driving force (DF_{GABA}) was estimated by the exponential fit of the *I–V* curve. (B) All-points histograms from 2 min of recording at $V_p = -80$ mV.

15 ± 3 mV; $n = 12$). Calculated for each cell, E_{GABA} was within the range from −44 mV to −74 mV (mean, −58 ± 3 mV; $n = 12$). In the age group P21–P28, three interneurons were recorded and morphologically identified in CA3 stratum radiatum ($n = 2$) and stratum oriens ($n = 1$). In these cells, E_m was −66 ± 1 mV, DF_{GABA} was −3 ± 1 mV, and E_{GABA} was −69 ± 1 mV ($n = 3$). Thus, during postnatal development, somatic GABA action shifts from depolarizing to slightly hyperpolarizing in the majority of hippocampal interneurons.

E_{GABA} *in CA3 pyramidal cells in the superfused hippocampus* in vivo

Recordings from the hippocampal pyramidal cells were also performed *in vivo* using a superfused hippocampus preparation, in which the cortex above the CA3 and CA1 hippocampus is removed and the hippocampal surface is continuously superfused with ACSF (Khazipov & Holmes, 2003). Cell-attached recordings of GABA(A) and NMDA channels were performed from the putative pyramidal

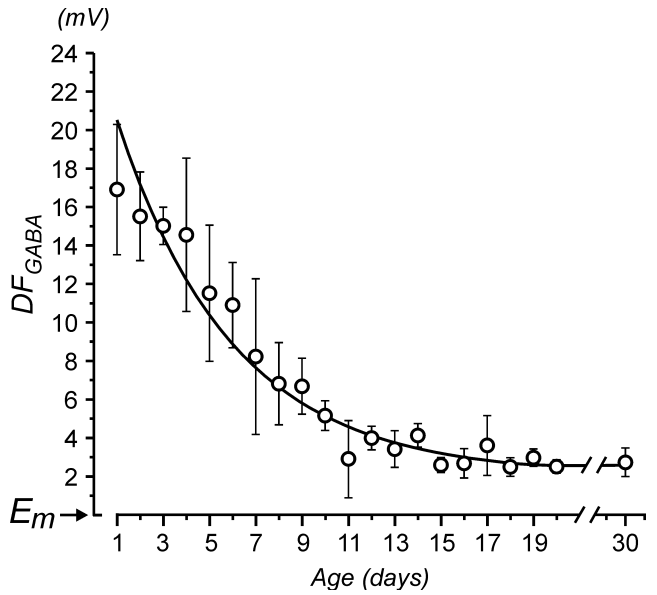

FIG. 4. Postnatal changes in the somatic γ-aminobutyric acid (GABA)(A) driving force (DF_{GABA}) in hippocampal neurons. Summary plot of the age dependence of DF_{GABA} estimated using cell-attached recordings of single GABA(A) channels (from 165 CA3 pyramidal cells). Note that DF_{GABA} is strongly depolarizing during the first postnatal week and progressively shifts to less depolarizing values during maturation, but does not switch to hyperpolarizing relative to the resting membrane potential (E_m).

cells at a depth of 150–200 μm from the hippocampal surface, which corresponds to the pyramidal cell layer (Figs 6 and 7). In P4–P5 rat pups, E_m of pyramidal cells was −70 ± 4 mV (range −61 to −81 mV; n = 5), and DF_{GABA} was 11 ± 3 mV (range 2–22 mV; n = 7). In P19–P40 pyramidal cells, E_m was −76 ± 4 mV (range −61 to −91 mV; n = 8), and DF_{GABA} was 4 ± 1 mV (range −1 to 13 mV; n = 14). Resulting values for E_{GABA} were −59 mV and −72 mV in the neonatal and adult pyramidal cells, respectively. These are similar to the values obtained in the hippocampal slices *in vitro*, suggesting that the developmental changes in chloride homeostasis and actions of GABA, which have been previously studied using *in vitro* preparations, reflect the physiological phenomenon.

Depolarizing action of GABA in adult CA3 pyramidal cells

Despite a high level of expression of chloride-extrusion transporters, which should set E_{GABA} at hyperpolarizing values, GABA responses are slightly depolarizing in adult pyramidal neurons. One explanation of this paradox involves the permeability of GABA(A) channels to bicarbonate ions. Although the permeability to bicarbonate ions is relatively low [about 0.2–0.4 when compared with chloride ions (Bormann *et al.*, 1987; Fatima-Shad & Barry, 1993; Kaila, 1994)], the bicarbonate equilibrium potential is set at around −10 mV, and therefore the driving force for bicarbonate ions (∼70 mV) is much greater than that for chloride ions, and so the current through GABA receptors at rest is predominantly mediated by bicarbonate ions (Kaila *et al.*, 1993; Kaila, 1994). To estimate the bicarbonate contribution to the depolarizing action of GABA in adult neurons, we measured the effect of removal of bicarbonate ions using Hepes-buffered, CO_2/HCO_3-free extracellular solution saturated with O_2 on DF_{GABA} measured using cell-attached recordings of GABA(A) channels from 1-month-old rat CA3 pyramidal cells. In control conditions in this series (in the bicarbonate-based ACSF), DF_{GABA} was 1.9 ± 0.6 mV (n = 9). In bicarbonate-free Hepes-buffered solution, DF_{GABA} was −3.7 ± 1.8 mV (n = 10; $P < 0.05$; Fig. 8A). These results indicate that bicarbonate conductance significantly contributes to DF_{GABA} in the soma of adult CA3 pyramidal cells. Subtraction of the bicarbonate component allows an estimation of the chloride equilibrium potential in the soma of adult CA3 pyramidal cells at around −82 mV. Assuming $[HCO_3^-]_I = 16$ mM and that the relative permeability $HCO_3^-/Cl^- = 0.2$, we further estimated $[Cl^-]_i$ according to the Goldman equation:

$$E_{GABA} = RT/F \ln[([Cl^-]_i + 0.2 \cdot [HCO_3^-]_i)/([Cl^-]_o + 0.2 \cdot [HCO_3^-]_o)]$$

We estimated $[Cl^-]_i$ in the soma of adult pyramidal cells as 4 mM, which corresponds to a $[Cl^-]_i$ equilibrium potential of −91 mV. This theoretical value is more negative than the value obtained in the bicarbonate-free Hepes-buffered ACSF (−82 mV). The difference is probably due to residual intracellular bicarbonate ions in the Hepes-buffered ACSF.

Another mechanism contributing to depolarizing GABA may involve activity of the chloride loader NKCC1. Although NKCC1 expression dramatically reduces with maturation, significant levels of NKCC1 expression can be detected even in adult neurons (Dzhala *et al.*, 2005). We therefore tested the effect of bumetanide, which is a highly selective NKCC1 antagonist at doses < 20 μM, on DF_{GABA} in adult neurons. We found that bumetanide (10 μM) strongly shifted DF_{GABA} from 1.0 ± 1.2 mV to −8.1 ± 2.2 mV (n = 10; $P < 0.05$) in 1-month-old CA3 pyramidal neurons (Fig. 8B). According to the Goldman equation, the effect of bumetanide is associated with a reduction of $[Cl^-]_i$ from 4 to 2 mM. Taken together, these results indicate that DF_{GABA} in the soma of adult CA3 pyramidal cells is set at slightly depolarizing values by an equilibrium between chloride-extrusion and chloride-loading systems and bicarbonate permeability of GABA(A) receptor channels.

Discussion

In this study, we examined the postnatal changes in GABA driving force and reversal potential in the somatic region of CA3 pyramidal cells using noninvasive cell-attached recordings of single channels. The major findings of the present study are that: (i) the postnatal E–I switch in the action of GABA on CA3 pyramidal cells is not associated with a change in the polarity of the GABAergic responses; and (ii) in adult hippocampal pyramidal cells, somatic GABA responses are slightly depolarizing, with somatic E_{GABA} being set by chloride extrusion, NKCC1-based chloride loading, and bicarbonate conductance.

The classic view of the developmental switch in the action of GABA from excitatory to inhibitory is that it is due to a switch in the polarity of GABA responses from depolarizing to hyperpolarizing. Although the results of the present study confirm that the excitatory action of GABA is due to its depolarizing effects on immature neurons, they also suggest that the postnatal E–I switch in the action of GABA is not associated with a switch in the polarity of GABA responses to hyperpolarizing. The developmental profile of the E–I switches, DF_{GABA} and the two determining parameters, E_{GABA} and E_m, are summarized in Fig. 9. In this study, using cell-attached recordings of GABA channels, we found that GABA strongly (by 10–20 mV) depolarizes CA3 pyramidal cells during the postnatal period, when GABA is excitatory, that the amplitude of this

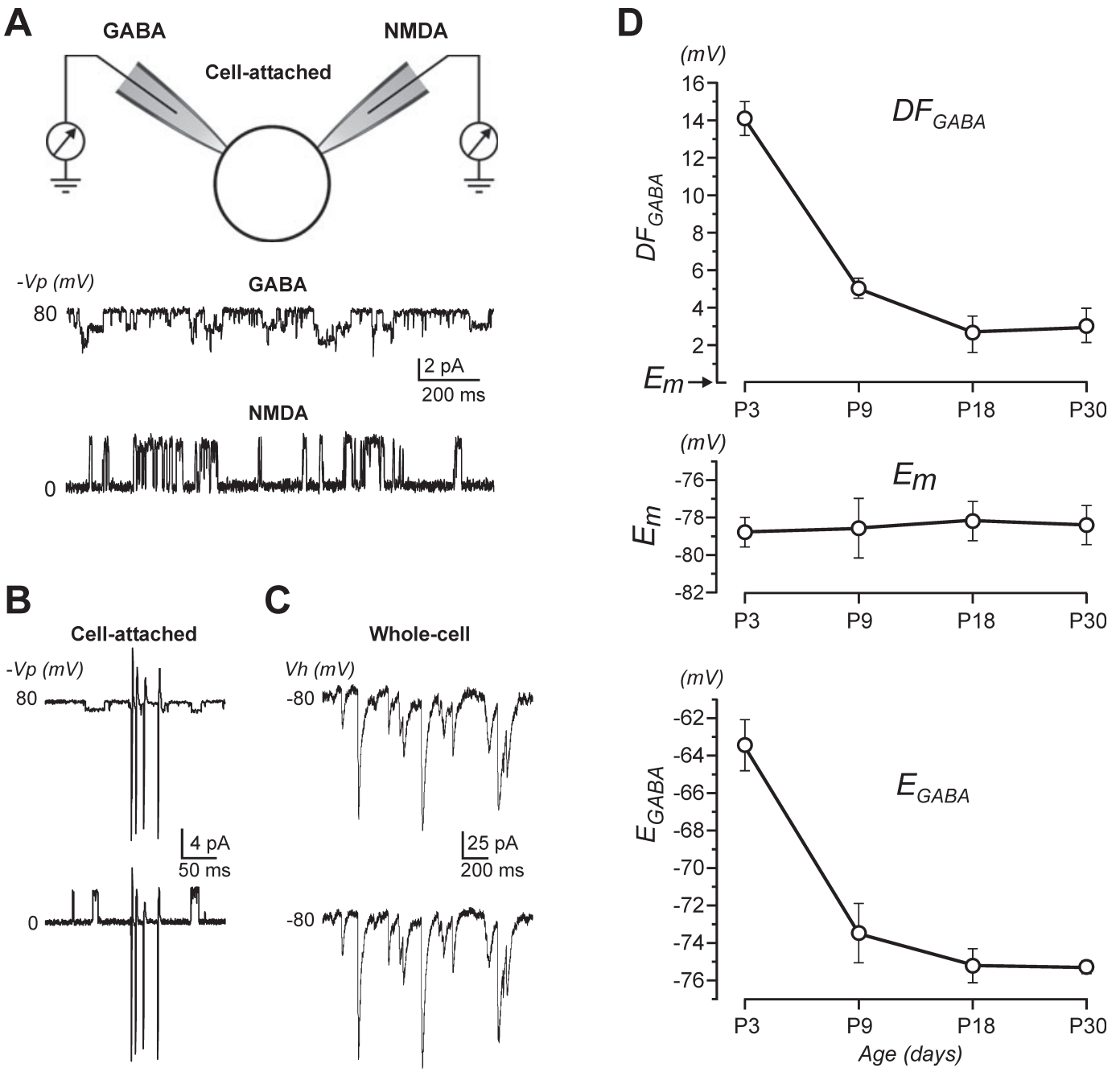

FIG. 5. Dual recordings of single γ-aminobutyric acid (GABA)(A) and NMDA channels. (A) Scheme of the dual cell-attached recordings of single GABA(A) and *N*-methyl-D-aspartate (NMDA) channels from a CA3 pyramidal cell. Representative traces of dual recordings are shown below. Spontaneous bursts of action potentials in cell-attached recordings (B) and synaptic activity recorded in whole-cell configuration (C) occur simultaneously in both electrodes, confirming that the recordings were performed from the same cell. (D) Summary plots of GABA(A) driving force (DF_{GABA}) inferred from *I–V* curves of single GABA(A) channels (upper plot); resting membrane potential inferred from *I–V* curves of single NMDA channels (E_m, middle plot); and the GABA(A) reversal potential ($E_{GABA} = DF_{GABA} + E_m$; bottom plot). Pooled data from 43 CA3 pyramidal cells. Note that E_m does not change during postnatal development, and that depolarizing E_{GABA} shifts negatively during development but does not reach the value of E_m. P, postnatal day; V_p, pipette potential.

depolarization progressively reduces during the two postnatal weeks, and that the developmental changes in E_{GABA} underlie the postnatal reduction in DF_{GABA}. These findings are in general agreement with the results of previous studies. However, during the postnatal E–I switch, we did not observe the switch in the polarity of DF_{GABA} from depolarizing to hyperpolarizing that had been found previously using intracellular (Obata *et al.*, 1978; Mueller *et al.*, 1984; Ben-Ari *et al.*, 1989; Swann *et al.*, 1989; Luhmann & Prince, 1991; Psarropoulou & Descombes, 1999; Rivera *et al.*, 1999; Banke & McBain, 2006), gramicidin-perforated patch (Banke & McBain, 2006) and extracellular field potential recordings (Romo-Parra *et al.*, 2008). Instead, we found that by the time of the postnatal E–I switch, E_{GABA} reaches values close to E_m, and DF_{GABA} remains slightly depolarizing. This discrepancy is due to strong differences in the E_m estimations (Fig. 9C). In the current study, using cell-attached recordings of NMDA channels as voltage sensors, we found that E_m values at the

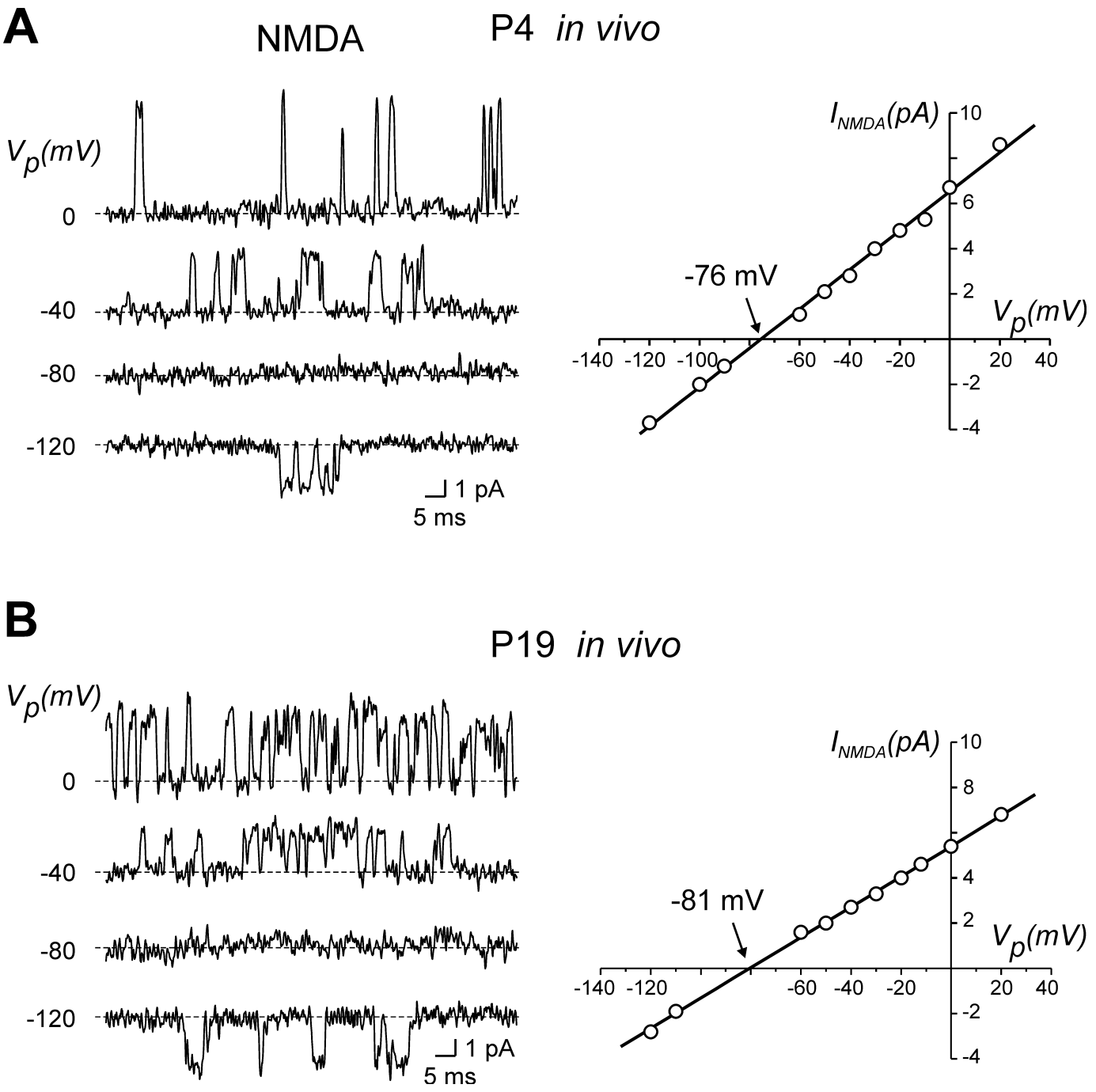

FIG. 6. Estimation of the resting membrane potential using cell-attached recordings of *N*-methyl-D-aspartate (NMDA) channels in the superfused hippocampus *in vivo*. Cell-attached recordings of the currents via single NMDA channels in the pyramidal cells at different pipette potentials (V_p) at postnatal day (P)4 (A) and P19 (B). The dashed line indicates the closed state. In the right panels, corresponding *I–V* relationships are shown; deduced resting membrane potential (E_m) values are indicated by arrows. Recordings were obtained from the pyramidal cell layer using a superfused hippocampus preparation from urethane-anaesthetized rats.

moment of E–I switch are more negative (by 10–20 mV) than those obtained using conventional approaches, including intracellular, whole-cell and gramicidin-perforated patch recordings, and cell-attached recordings of potassium channels (Ben-Ari *et al.*, 1989; Rovira & Ben-Ari, 1993; Tyzio *et al.*, 2003; Banke & McBain, 2006). This raises the question of the reliability of E_m values obtained using cell-attached recordings of NMDA channels. The results of dual cell-attached NMDA channels and whole-cell recordings gave an estimation of the error of E_m measurements using NMDA channels of 0.9 ± 1.3 mV (Fig. 2), and confirmed that invasive recording techniques cause neuronal depolarization by introducing shunt conductance to the recorded cell [see also Barry & Lynch (1991), Fricker *et al.* (1999), Verheugen *et al.* (1999), Tyzio *et al.* (2003), Wang *et al.* (2003), Yamada *et al.* (2004), Mohajerani & Cherubini (2005), Esposito *et al.* (2005), Corder-Erausquin *et al.* (2005), Banke & McBain (2006), Perkins (2006), Ge *et al.* (2006), Achilles *et al.* (2007) and Marchionni *et al.* (2007)]. This depolarization is most evident in small immature neurons with high membrane resistance [Fig. 9C, and

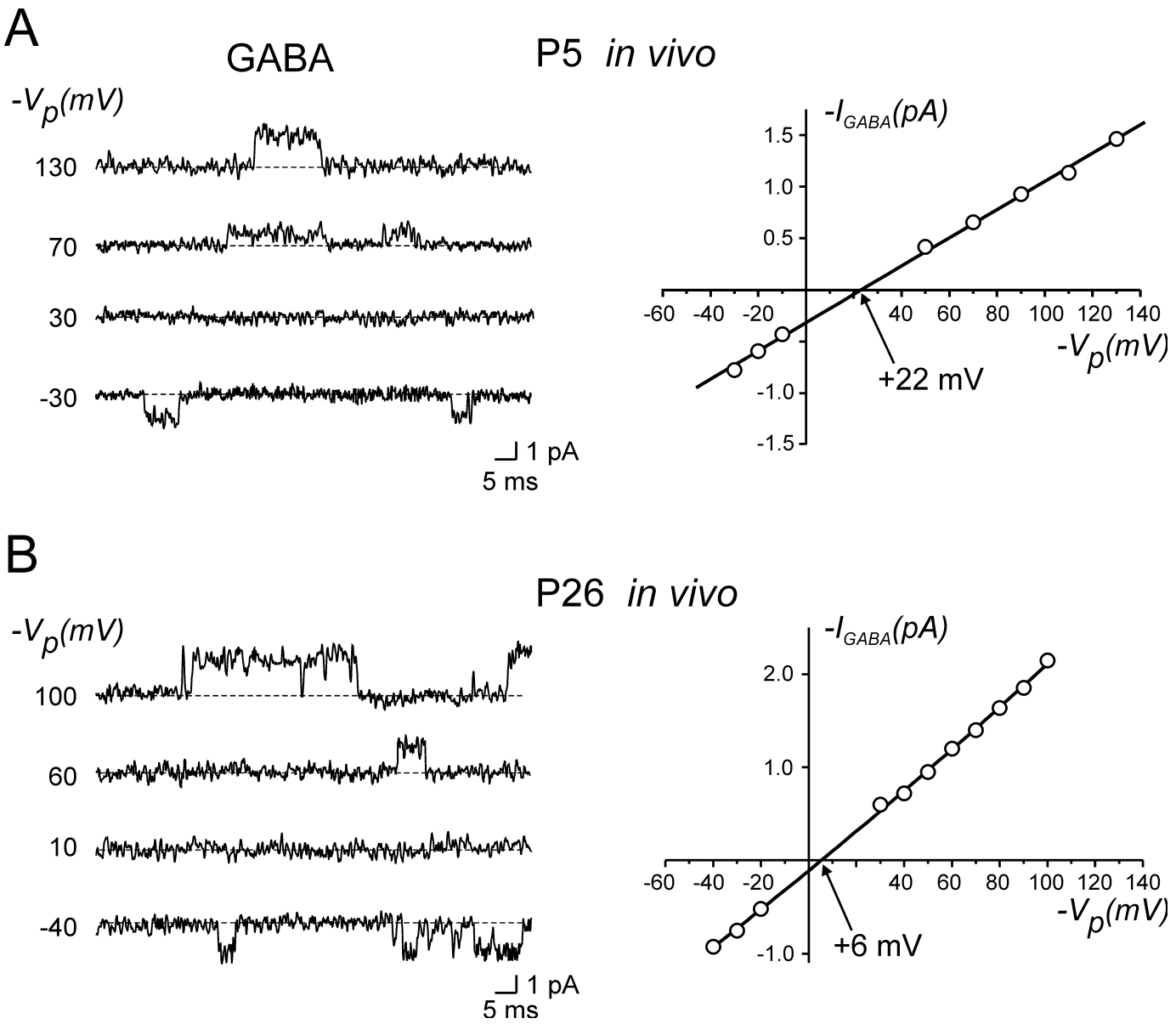

FIG. 7. Estimation of the γ-aminobutyric acid (GABA) driving force (DF_{GABA}) using cell-attached recordings of single GABA channels in the superfused hippocampus *in vivo*. Cell-attached recordings of the currents via single GABA channels in the pyramidal cells at different pipette potentials (V_p) at postnatal day (P)5 (A) and P26 (B). The dashed line indicates the closed state. In the right panels, corresponding *I–V* relationships are shown; DF_{GABA} values are indicated by arrows. The experimental setup was the same as in Fig. 6.

see also Tyzio *et al.* (2003, 2007)]. This is also in keeping with strongly negative E_m values of ≤ −80 mV obtained in acutely dissociated cortical neurons at embryonic stages (E11–E22) using noninvasive potentiometric techniques; with perforated patch recordings, E_m was −60 mV, i.e. 20–25 mV more depolarized (Maric *et al.*, 1998). Artificial neuronal depolarization could explain apparently hyperpolarizing DF_{GABA} despite depolarized E_{GABA} in some perforated patch and intracellular recordings during the postnatal period (Fig. 9C; [see also Rovira & Ben-Ari (1993) and Tyzio *et al.* (2003, 2007)] and in adult neurons. Indeed, neuronal depolarization by 10–13 mV is still introduced by whole-cell recordings of perforated patch recordings, even in adult pyramidal cells [Fig. 9; see also Fricker *et al.* (1999), Verheugen *et al.* (1999) and Tyzio *et al.* (2003)]. Interestingly, the estimates of E_{GABA} obtained using dual cell-attached and gramicidin-perforated patch recordings differ less than the estimates of DF_{GABA} or E_m [Fig. 9D; see also Tyzio *et al.* (2007)]. Therefore, the present results suggest that in adult CA3 pyramidal cells, which have been widely considered to be prototypes of neurons with 'classic' hyperpolarizing inhibitory postsynaptic potentials, somatic GABAergic inhibition is not hyperpolarizing but shunting. Shunting inhibition by depolarizing GABA has been previously suggested in different types of neurons (Eccles *et al.*, 1961; Barrett & Crill, 1974; Kennedy *et al.*, 1974; Misgeld *et al.*, 1986; Edwards, 1990; Staley & Mody, 1992; Kaila *et al.*, 1993; Zhang & Jackson, 1993; Golding & Oertel, 1996; Cattaert & El Manira, 1999; Rudomin & Schmidt, 1999; Lu & Trussell, 2001; Martina *et al.*, 2001; Monsivais & Rubel, 2001; Bartos *et al.*, 2002; Chavas & Marty, 2003; Gulledge & Stuart, 2003; Banke & McBain, 2006; Vida *et al.*, 2006). Purely shunting GABAergic inhibition may be more advantageous than hyperpolarizing inhibition, because of its low metabolic cost (Buzsaki *et al.*, 2007) and absence of hyperpolarization-

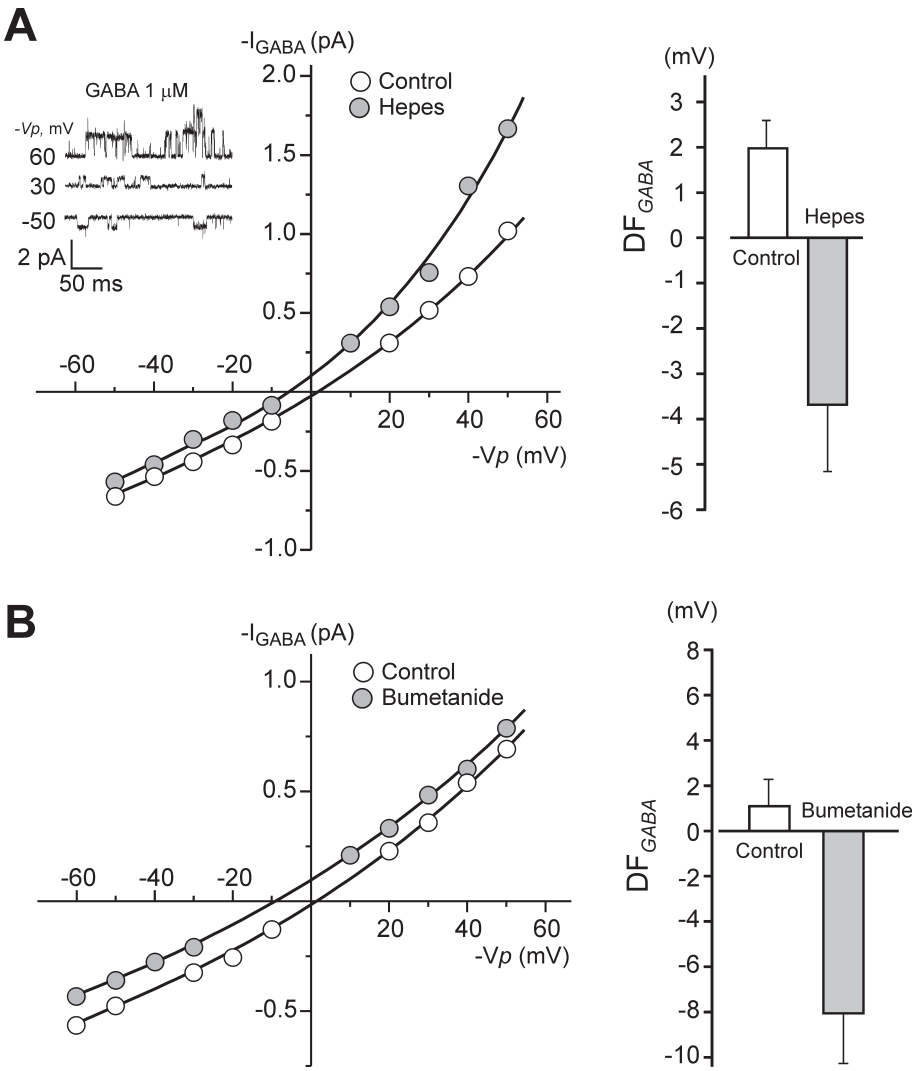

FIG. 8. Contributions of bicarbonate conductance and bumetanide-sensitive chloride transport to the γ-aminobutyric acid (GABA) responses in adult pyramidal cells. Cell-attached recordings of GABA channels (inset) and corresponding *I–V* relationships in control conditions (open circles), after 30 min of perfusion with bicarbonate-free Hepes-based artificial cerebrospinal fluid (ACSF; A, filled circles), and in the presence of bumetanide (10 μM; B, filled circles). Group data are shown in the right panels. Recordings from P28–P30 CA3 pyramidal cells *in vitro*. V_p, pipette potential.

triggered excitation (Llinas & Muhlethaler, 1988; Bal *et al.*, 1995; Aizenman & Linden, 1999).

The present findings of depolarizing GABA in adult CA3 pyramidal cells are in contrast to results obtained using extracellular local field potential recordings. It has been recently shown that activation of somatic GABA(A) receptors by synaptic stimulation or by application of a GABA(A) receptor agonist induces depolarizing responses in immature neurons and hyperpolarizing responses in adult CA3 pyramidal neurons, with a switch from depolarization to hyperpolarization occurring during the second postnatal week (Romo-Parra *et al.*, 2008). The reasons for the discrepancy are not understood, and they may involve methodological differences such as the use of an immersed vs. interphase recording chamber and ACSF composition. In future experiments, it will be important to compare the polarity of GABA responses under similar experimental conditions using cell-attached recordings of GABA channels and local field potential responses to GABA.

Developmental changes in GABA signalling are due to the age-dependent expression of the transporters and channels that regulate intracellular chloride homeostasis (Payne *et al.*, 2003; Ben Ari *et al.*, 2007; Farrant & Kaila, 2007). Considerable evidence indicates that high-level expression of the chloride loader NKCC1 and low-level expression of the chloride extruder KCC2 determines elevated $[Cl^-]_i$ in neonatal hippocampal pyramidal cells, and that progressive loss of NKCC1 and expression of KCC2 are the two major factors determining the postnatal $[Cl^-]_i$ reduction, as estimated here in the soma of CA3 from 15 mM at P1 to 4 mM at P15 and onwards. Our results indicate that in adult pyramidal cells, somatic GABA responses are maintained slightly depolarizing by chloride loading by NKCC1, bicarbonate conductance, and the chloride-extrusion system. Although previous studies indicated a developmental decline in NKCC1 expression, the results of the present study indicate the presence of a bumetanide-sensitive NKCC1-mediated chloride-loading mechanism in soma of adult CA3 pyramidal cells. This is compatible with the findings of depolarizing responses to GABA in the initial axon hillock (Szabadics *et al.*, 2006), and their bumetanide sensitivity (Khirug *et al.*, 2008). On the other hand, bumetanide negatively shifts E_{GABA} in adult interneurons (Banke & McBain, 2006) but not in

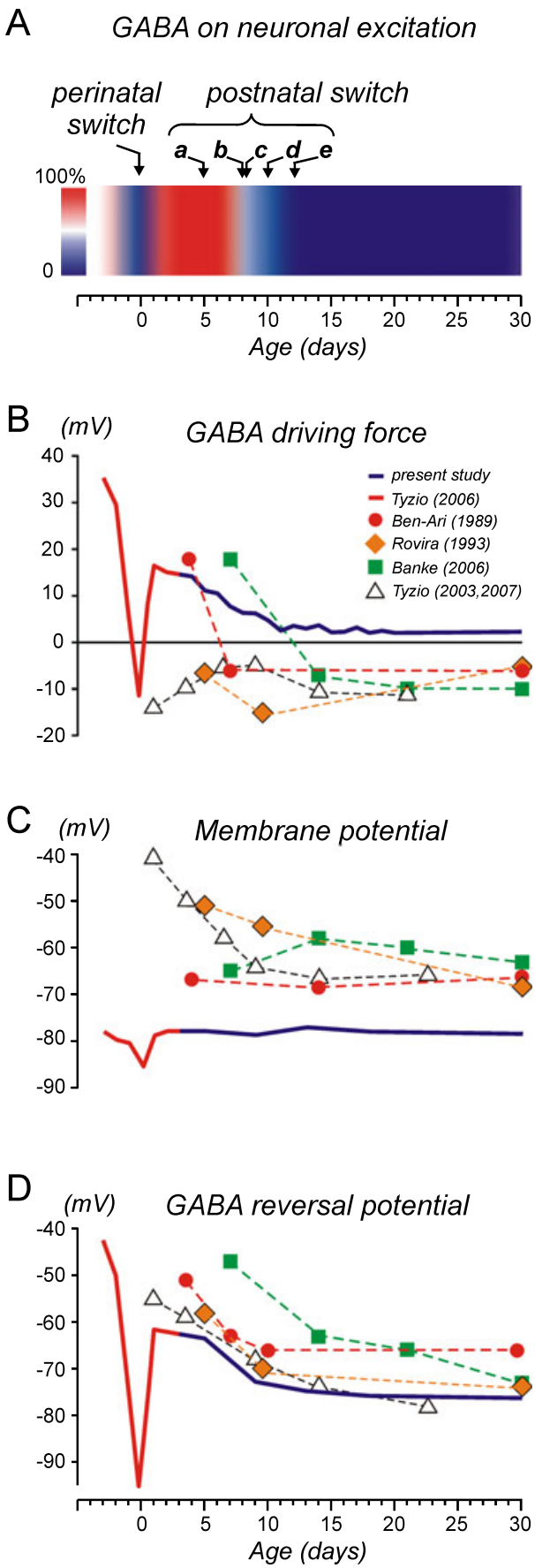

pyramidal cells (Banke & McBain, 2006; Romo-Parra *et al.*, 2008) in the CA3 hippocampus, and in the neocortex and amygdala (Martina *et al.*, 2001). A second factor contributing to depolarizing GABA responses is bicarbonate conductance of GABA(A) receptor channels (Bormann *et al.*, 1987; Fatima-Shad & Barry, 1993; Kaila, 1994). Hyperpolarizing GABA revealed in a bicarbonate-free medium and in the presence of bumetanide indicates powerful chloride-extrusion mechanisms, including potassium–chloride cotransporters in adult pyramidal cells (Zhang *et al.*, 1991; Plotkin *et al.*, 1997; Lu *et al.*, 1999; Rivera *et al.*, 1999; Ganguly *et al.*, 2001; Payne *et al.*, 2003; Mercado *et al.*, 2004; Yamada *et al.*, 2004; Dzhala *et al.*, 2005). However, unusually low estimates of $[Cl^-]_i$ (about 2 mM) obtained in the presence of bumetanide, as well as in bicarbonate-free medium and in the presence of oxytocin as reported previously (Tyzio *et al.*, 2006), cannot be achieved by potassium–chloride cotransport, which, at such low $[Cl^-]_i$, should operate as a chloride loader. These results indicate a contribution from another chloride-extrusion mechanism, which could be an Na^+-dependent anion exchanger (Grichtchenko *et al.*, 2001; Jacobs *et al.*, 2008) or another as yet non-identified transporter. Clearly, further studies are needed to clarify maturation of E_{GABA} and the factors determining chloride homeostasis in somatic and other cell compartments.

The present results suggest that somatic GABA responses are depolarizing in the majority of immature CA3 interneurons (from E_m −73 mV to E_{GABA} −58 mV). This is in agreement with the results of a study using cell-attached recordings of potassium channels from P1–P4 CA1 interneurons, which reported that activation of GABA(A) receptors causes neuronal depolarization from −74 to −55 mV (Verheugen *et al.*, 1999). Similarly, synaptic activation of GABA(A) receptors caused an increase in $[Ca^{2+}]_i$ (Leinekugel *et al.*, 1995) and generated action potentials in cell-attached recordings (Khazipov *et al.*, 1997) in P2–P5 CA3 interneurons. In the postnatal neocortex, activation of GABA(A) receptors caused an increase in GABAergic

FIG. 9. Developmental profile of somatic γ-aminobutyric acid (GABA) signalling in hippocampal CA3 pyramidal neurons. (A) Excitatory-to-inhibitory (E–I) developmental switches in the action of GABA on Wistar rat hippocampal CA3 pyramidal cells were estimated by pooling the results of cell-attached and gramicidin-perforated patch recordings (Tyzio *et al.*, 2006, 2007); the colour code indicates the proportion of cells with excitatory GABA. Note the first transient switch near term and the second permanent switch during the second postnatal week. Arrows (a to e) indicate the estimates of the second permanent E–I switch obtained using different methodological approaches: (a) at postnatal day (P)5, using sharp electrodes (Ben-Ari *et al.*, 1989; Swann *et al.*, 1989); (b) at P8, using extracellular multiple unit activity (MUA) recordings and synaptic activation of GABA(A) receptors (Tyzio *et al.*, 2007); (c) at P8, using gramicidin-perforated patch recordings (Tyzio *et al.*, 2007); (d) at P10, using MUA recordings and brief bath application of the GABA(A) agonist isoguvacine (Tyzio *et al.*, 2007) [at P13 in Sprague–Dawley rats (Khazipov *et al.*, 2004)]; (e) at P12, using MUA recordings and the GABA(A) antagonist bicuculline (Dzhala & Staley, 2003). Estimates of the E–I switch obtained using $[Ca^{2+}]_i$ imaging techniques also placed it between P5 and P12 (Leinekugel *et al.*, 1995; Garaschuk *et al.*, 1998). (B–D) Developmental changes in the GABA driving force (DF_{GABA}), resting membrane potential (E_m) and GABA(A) reversal potential (E_{GABA}) in CA3 pyramidal cells inferred from cell-attached recordings of single GABA and *N*-methyl-D-aspartate (NMDA) channels, and from the results obtained using intracellular (Ben-Ari *et al.*, 1989; Rovira & Ben-Ari, 1993), gramicidin-perforated patch (Banke & McBain, 2006; Tyzio *et al.*, 2007) and cell-attached recordings of potassium channels (Banke & McBain, 2006). Results of single and dual recordings of GABA and NMDA channels during the postnatal period are pooled together, and the values for the fetal and near-term period are taken from Tyzio *et al.* (2006). The results of the present study indicate that the postnatal E–I switch occurs without a change in the polarity of GABA signals.

synaptic activity, which also indicated an excitatory effect of GABA on interneurons (Owens *et al.*, 1999). These results indicate depolarizing and excitatory actions of GABA in the immature interneurons. However, the interneuron population is highly heterogeneous (Freund & Buzsaki, 1996), and the action of GABA may be interneuron cell-type dependent. Indeed, a developmental study in the stratum lucidum interneurons revealed slightly hyperpolarizing synaptic GABA responses in P5–P10 interneurons (Banke & McBain, 2006), with E_m of −63 mV (estimated using cell-attached recordings of potassium channels) and E_{GABA} of −66 mV (measured using gramicidin-perforated patch). On the other hand, it has been demonstrated that GABA depolarizes and excites neuropeptide Y hilar interneurons in adult mice (Fu & van den Pol, 2007). Thus, although the developmental rule of a transient depolarizing and excitatory action of GABA in the immature cells involves the majority of interneurons, cell-type specificity may exist.

The results obtained using superfused hippocampus preparations *in vivo* indicate that the developmental changes in GABA signalling also take place *in vivo*. In particular, we found that E_{GABA} shifts from −59 mV during the first postnatal week to −72 mV in adult hippocampal pyramidal cells, values that are close to those obtained *in vitro*. Because these recordings were obtained under anaesthesia, it can be suggested that the present results, including depolarizing GABA in adult cells, may be relevant to deep sleep, when neurons are relatively hyperpolarized, as in slices *in vitro*. During waking and rapid eye movement sleep, when neurons are in a more depolarized state, GABA may switch its action and become hyperpolarizing.

In conclusion, the noninvasive study of the developmental changes in GABA signalling revealed that the postnatal developmental switch in the action of GABA from excitatory to inhibitory is not associated with a switch in the polarity of the GABAergic responses from depolarizing to hyperpolarizing that has been consistently reported in earlier studies using intracellular recordings. Instead, there is a progressive developmental shift of the GABA(A) reversal potential from strongly depolarizing to slightly depolarizing values, so that even in adult hippocampal pyramidal cells, GABA provides shunting, but not hyperpolarizing, inhibition.

Acknowledgements

We thank Professor P. H. Barry for the helpful suggestions, and Drs K. Kaila, C. Hammond, I. Medina and M. Colonnese for helpful comments on the manuscript. This work was supported by INSERM, Fondation pour la Recherche Médicale, International Brain Research Organization, L'Agence Nationale de la Recherche, and European Community grant LSHB-CT-2004-503467.

Abbreviations

ACSF, artificial cerebrospinal fluid; DF_{GABA}, GABA(A) driving force; E_{GABA}, GABA(A) reversal potential; E–I, excitatory-to-inhibitory; E_m, resting membrane potential; GABA, γ-aminobutyric acid; NMDA, *N*-methyl-D-aspartate; P, postnatal day; PBS, phosphate-buffered saline; V_p, pipette potential.

References

Achilles, K., Okabe, A., Ikeda, M., Shimizu-Okabe, C., Yamada, J., Fukuda, A., Luhmann, H.J. & Kilb, W. (2007) Kinetic properties of Cl-uptake mediated by Na^+-dependent K^+-2Cl(−) cotransport in immature rat neocortical neurons. *J. Neurosci.*, **27**, 8616–8627.

Aizenman, C.D. & Linden, D.J. (1999) Regulation of the rebound depolarization and spontaneous firing patterns of deep nuclear neurons in slices of rat cerebellum. *J. Neurophysiol.*, **82**, 1697–1709.

Bal, T., von Krosigk, M. & McCormick, D.A. (1995) Synaptic and membrane mechanisms underlying synchronized oscillations in the ferret lateral geniculate nucleus in vitro. *J. Physiol. (Lond.)*, **483**, 641–663.

Banke, T.G. & McBain, C.J. (2006) GABAergic input onto CA3 hippocampal interneurons remains shunting throughout development. *J. Neurosci.*, **26**, 11720–11725.

Barrett, J.N. & Crill, W.E. (1974) Specific membrane properties of cat motoneurones. *J. Physiol.*, **239**, 301–324.

Barry, P.H. & Lynch, J.W. (1991) Liquid junction potentials and small cell effects in patch-clamp analysis. *J. Membr. Biol.*, **121**, 101–117.

Bartos, M., Vida, I., Frotscher, M., Meyer, A., Monyer, H., Geiger, J.R.P. & Jonas, P. (2002) Fast synaptic inhibition promotes synchronized gamma oscillations in hippocampal interneuron networks. *Proc. Natl Acad. Sci. USA*, **99**, 13222–13227.

Ben Ari, Y. (2002) Excitatory actions of GABA during development: the nature of the nurture. *Nat. Rev. Neurosci.*, **3**, 728–739.

Ben Ari, Y., Gaiarsa, J.L., Tyzio, R. & Khazipov, R. (2007) GABA: a pioneer transmitter that excites immature neurons and generates primitive oscillations. *Physiol. Rev.*, **87**, 1215–1284.

Ben-Ari, Y., Cherubini, E., Corradetti, R. & Gaïarsa, J.-L. (1989) Giant synaptic potentials in immature rat CA3 hippocampal neurones. *J. Physiol. (Lond.)*, **416**, 303–325.

Ben-Ari, Y., Khazipov, R., Leinekugel, X., Caillard, O. & Gaïarsa, J.-L. (1997) $GABA_A$, NMDA and AMPA receptors: a developmentally regulated 'ménage a trois'. *Trends Neurosci.*, **20**, 523–529.

Bormann, J., Hamill, O.P. & Sakmann, B. (1987) Mechanisms of anion permeation through channels gated by glycine and g-aminobutyric acid in mouse cultured spinal neurones. *J. Physiol. (Lond.)*, **385**, 243–286.

Buzsaki, G., Kaila, K. & Raichle, M. (2007) Inhibition and brain work. *Neuron*, **56**, 771–783.

Cattaert, D. & El Manira, A. (1999) Shunting versus inactivation: analysis of presynaptic inhibitory mechanisms in primary afferents of the crayfish. *J. Neurosci.*, **19**, 6079–6089.

Chavas, J. & Marty, A. (2003) Coexistence of excitatory and inhibitory GABA synapses in the cerebellar interneuron network. *J. Neurosci.*, **23**, 2019–2031.

Cherubini, E., Gaïarsa, J.-L. & Ben-Ari, Y. (1991) GABA: an excitatory transmitter in early postnatal life. *Trends Neurosci.*, **14**, 515–519.

Corder-Erausquin, M., Coull, J.A.M., Boudreau, D., Rolland, M. & de Koninck, Y. (2005) Differential maturation of GABA action and anion reversal potential in spinal lamina I neurons: impact of chloride extrusion capacity. *J. Neurosci.*, **25**, 9613–9623.

Dzhala, V.I. & Staley, K.J. (2003) Excitatory actions of endogenously released GABA contribute to initiation of ictal epileptiform activity in the developing hippocampus. *J. Neurosci.*, **23**, 1840–1846.

Dzhala, V.I., Talos, D.M., Sdrulla, D.A., Brumback, A.C., Mathews, G.C., Benke, T.A., Delpire, E., Jensen, F.E. & Staley, K.J. (2005) NKCC1 transporter facilitates seizures in the developing brain. *Nat. Med.*, **11**, 1205–1213.

Eccles, J.C., Eccles, R.M. & Magni, F. (1961) Central inhibitory action attributable to presynaptic depolarization produced by muscle afferent volleys. *J. Physiol.*, **159**, 147–166.

Edwards, D.H. (1990) Mechanisms of depolarizing inhibition at the crayfish giant motor synapse. 1 Electrophysiology. *J. Neurophysiol.*, **64**, 532–540.

Esposito, M.S., Piatti, V.C., Laplagne, D.A., Morgenstern, N.A., Ferrari, C.C., Pitossi, F.J. & Schinder, A.F. (2005) Neuronal differentiation in the adult hippocampus recapitulates embryonic development. *J. Neurosci.*, **25**, 10074–10086.

Farrant, M. & Kaila, K. (2007) The cellular, molecular and ionic basis of GABA(A) receptor signalling [In *GABA and the Basal Ganglia: from Molecules to Systems*.]. *Prog. Brain Res.*, **160**, 59–87.

Fatima-Shad, K. & Barry, P.H. (1993) Anion permeation in GABA- and glycine-gated channels of mammalian cultured hippocampal neurons. *Proc. Biol. Sci.*, **253**, 69–75.

Fiumelli, H. & Woodin, M.A. (2007) Role of activity-dependent regulation of neuronal chloride homeostasis in development. *Curr. Opin. Neurobiol.*, **17**, 81–86.

Freund, T. & Buzsaki, G. (1996) Interneurons of the hippocampus. *Hippocampus*, **6**, 345–470.

Fricker, D., Verheugen, J.A. & Miles, R. (1999) Cell-attached measurements of the firing threshold of rat hippocampal neurones. *J. Physiol.*, **517**, 791–804.

Fu, L.Y. & van den Pol, A.N. (2007) GABA excitation in hilar neuropeptide Y neurons. *J. Physiol.*, **579**, 445–464.

Ganguly, K., Schinder, A.F., Wong, S.T. & Poo, M.M. (2001) GABA itself promotes the developmental switch of neuronal GABAergic responses from excitation to inhibition. *Neuron*, **105**, 521–532.

Garaschuk, O., Hanse, E. & Konnerth, A. (1998) Developmental profile and synaptic origin of early network oscillations in the CA1 region of rat neonatal hippocampus. *J. Physiol. (Lond.)*, **507**, 219–236.

Ge, S.Y., Goh, E.L.K., Sailor, K.A., Kitabatake, Y., Ming, G.L. & Song, H.J. (2006) GABA regulates synaptic integration of newly generated neurons in the adult brain. *Nature*, **439**, 589–593.

Golding, N.L. & Oertel, D. (1996) Context-dependent synaptic action of glycinergic and GABAergic inputs in the dorsal cochlear nucleus. *J. Neurosci.*, **16**, 2208–2219.

Grichtchenko, I.I., Choi, I.Y., Zhong, X.B., Bray-Ward, P., Russell, J.M. & Boron, W.F. (2001) Cloning, characterization, and chromosomal mapping of a human electroneutral Na^+-driven Cl-NCO3 exchanger. *J. Biol. Chem.*, **276**, 8358–8363.

Gulledge, A.T. & Stuart, G.J. (2003) Excitatory actions of GABA in the cortex. *Neuron*, **37**, 299–309.

Hara, M., Inoue, M., Yasukura, T., Ohnishi, S., Mikami, Y. & Inagaki, C. (1992) Uneven distribution of intracellular Cl^- in rat hippocampal neurons. *Neurosci. Lett.*, **143**, 135–138.

Jacobs, S., Ruusuvuori, E., Sipila, S.T., Haapanen, A., Damkier, H.H., Kurth, I., Hentschke, M., Schweizer, M., Rudhard, Y., Laatikainen, L.M., Tyynela, J., Praetorius, J., Voipio, J. & Hubner, C.A. (2008) Mice with targeted Slc4a10 gene disruption have small brain ventricles and show reduced neuronal excitability. *Proc. Natl Acad. Sci. USA*, **105**, 311–316.

Kaila, K. (1994) Ionic basis of GABAA receptor channel function in the nervous system. *Prog. Neurobiol.*, **42**, 489–537.

Kaila, K., Voipio, J., Paalasmaa, P., Pasternack, M. & Deisz, R.A. (1993) The role of bicarbonate in GABAA receptor-mediated IPSPs of rat neocortical neurones. *J. Physiol.*, **464**, 273–289.

Kennedy, D., Calabrese, R.L. & Wine, J.J. (1974) Presynaptic inhibition: primary afferent depolarization in crayfish neurons. *Science*, **186**, 451–454.

Khazipov, R. & Holmes, G.L. (2003) Synchronization of kainate-induced epileptic activity via GABAergic inhibition in the superfused rat hippocampus in vivo. *J. Neurosci.*, **23**, 5337–5341.

Khazipov, R., Ragozzino, D. & Bregestovski, P. (1995) Kinetics and Mg^{2+}block of *N*-methyl-D-aspartate receptor channels during postnatal development of hippocampal CA3 pyramidal neurons. *Neuroscience*, **69**, 1057–1065.

Khazipov, R., Leinekugel, X., Khalilov, I., Gaïarsa, J.-L. & Ben-Ari, Y. (1997) Synchronization of GABAergic interneuronal network in CA3 subfield of neonatal rat hippocampal slices. *J. Physiol. (Lond.)*, **498**, 763–772.

Khazipov, R., Esclapez, M., Caillard, O., Bernard, C., Khalilov, I., Tyzio, R., Hirsch, J., Dzhala, V., Berger, B. & Ben-Ari, Y. (2001) Early development of neuronal activity in the primate hippocampus in utero. *J. Neurosci.*, **21**, 9770–9781.

Khazipov, R., Khalilov, I., Tyzio, R., Morozova, E., Ben Ari, Y. & Holmes, G.L. (2004) Developmental changes in GABAergic actions and seizure susceptibility in the rat hippocampus. *Eur. J. Neurosci.*, **19**, 590–600.

Khirug, S., Yamada, J., Afzalov, R., Voipio, J., Khiroug, L. & Kaila, K. (2008) GABAergic depolarization of the axon initial segment in cortical principal neurons is caused by the Na-K-2Cl cotransporter NKCC1. *J. Neurosci.*, **28**, 4635–4639.

Leinekugel, X., Tseeb, V., Ben-Ari, Y. & Bregestovski, P. (1995) Synaptic $GABA_A$ activation induces Ca^{2+}rise in pyramidal cells and interneurons from rat neonatal hippocampal slices. *J. Physiol. (Lond.)*, **487**, 319–329.

Leinekugel, X., Medina, I., Khalilov, I., Ben-Ari, Y. & Khazipov, R. (1997) Ca^{2+}oscillations mediated by the synergistic excitatory actions of $GABA_A$ and NMDA receptors in the neonatal hippocampus. *Neuron*, **18**, 243–255.

Leinekugel, X., Khazipov, R., Cannon, R., Hirase, H., Ben Ari, Y. & Buzsaki, G. (2002) Correlated bursts of activity in the neonatal hippocampus in vivo. *Science*, **296**, 2049–2052.

Llinas, R. & Muhlethaler, M. (1988) Electrophysiology of guinea-pig cerebellar nuclear cells in the in vitro brain stem-cerebellar preparation. *J. Physiol. (Lond.)*, **404**, 241–258.

Lu, T. & Trussell, L.O. (2001) Mixed excitatory and inhibitory GABA-mediated transmission in chick cochlear nucleus. *J. Physiol.*, **535**, 125–131.

Lu, J., Karadsheh, M. & Delpire, E. (1999) Developmental regulation of the neuronal-specific isoform of K–Cl cotransporter KCC2 in postnatal rat brains. *J. Neurobiol.*, **39**, 558–568.

Luhmann, H.J. & Prince, D.A. (1991) Postnatal maturation of the GABAergic system in rat neocortex. *J. Neurophysiol.*, **65**, 247–263.

Marchionni, I., Omrani, A. & Cherubini, E. (2007) In the developing rat hippocampus a tonic GABA(A)-mediated conductance selectively enhances the glutamatergic drive of principal cells. *J. Physiol. (Lond.)*, **581**, 515–528.

Maric, D., Maric, I., Smith, S.V., Serafini, R., Hu, Q. & Barker, J.L. (1998) Potentiometric study of resting potential, contributing K^+ channels and the onset of Na^+ channel excitability in embryonic rat cortical cells. *Eur. J. Neurosci.*, **10**, 2532–2546.

Martina, M., Royer, S. & Pare, D. (2001) Cell-type-specific GABA responses and chloride homeostasis in the cortex and amygdala. *J. Neurophysiol.*, **86**, 2887–2895.

Marty, S., Wehrle, R., Alvarez-Leefmans, F.J., Gasnier, B. & Sotelo, C. (2002) Postnatal maturation of Na^+, K^+, $2Cl^-$ cotransporter expression and inhibitory synaptogenesis in the rat hippocampus: an immunocytochemical analysis. *Eur. J. Neurosci.*, **15**, 233–245.

Mercado, A., Mount, D.B. & Gamba, G. (2004) Electroneutral cation–chloride cotransporters in the central nervous system. *Neurochem. Res.*, **29**, 17–25.

Minlebaev, M., Ben-Ari, Y. & Khazipov, R. (2007) Network mechanisms of spindle-burst oscillations in the neonatal rat barrel cortex in vivo. *J. Neurophysiol.*, **97**, 692–700.

Misgeld, U., Deisz, R.A., Dodt, H.U. & Lux, H.D. (1986) The role of chloride transport in postsynaptic inhibition of hippocampal neurons. *Science*, **232**, 1413–1415.

Mohajerani, M.H. & Cherubini, E. (2005) Spontaneous recurrent network activity in organotypic rat hippocampal slices. *Eur. J. Neurosci.*, **22**, 107–118.

Monsivais, P. & Rubel, E.W. (2001) Accommodation enhances depolarizing inhibition in central neurons. *J. Neurosci.*, **21**, 7823–7830.

Mueller, A.L., Taube, J.S. & Schwartzkroin, P.A. (1984) Development of hyperpolarizing inhibitory postsynaptic potentials and hyperpolarizing response to gamma-aminobutyric acid in rabbit hippocampus studied in vitro. *J. Neurosci.*, **4**, 860–867.

Obata, K., Oide, M. & Tanaka, H. (1978) Excitatory and inhibitory actions of GABA and glycine on embryonic chick spinal neurons in culture. *Brain Res.*, **144**, 179–184.

Owens, D.F. & Kriegstein, A.R. (2002) Is there more to gaba than synaptic inhibition? *Nat. Rev. Neurosci.*, **3**, 715–727.

Owens, D.F., Liu, X. & Kriegstein, A.R. (1999) Changing properties of GABA(A) receptor-mediated signaling during early neocortical development. *J. Neurophysiol.*, **82**, 570–583.

Payne, J.A., Rivera, C., Voipio, J. & Kaila, K. (2003) Cation–chloride co-transporters in neuronal communication, development and trauma. *Trends Neurosci.*, **26**, 199–206.

Perkins, K.L. (2006) Cell-attached voltage-clamp and current-clamp recording and stimulation techniques in brain slices. *J. Neurosci. Methods*, **154**, 1–18.

Plotkin, M.D., Snyder, E.Y., Hebert, S.C. & Delpire, E. (1997) Expression of the Na-K-2Cl cotransporter is developmentally regulated in postnatal rat brains: a possible mechanism underlying GABA's excitatory role in immature brain. *J. Neurobiol.*, **33**, 781–795.

Psarropoulou, C. & Descombes, S. (1999) Differential bicuculline-induced epileptogenesis in rat neonatal, juvenile and adult CA3 pyramidal neurons in vitro. *Dev. Brain Res.*, **117**, 117–120.

Rivera, C., Voipio, J., Payne, J.A., Ruusuvuori, E., Lahtinen, H., Lamsa, K., Pirvola, U., Saarma, M. & Kaila, K. (1999) The K^+/Cl^- co-transporter KCC2 renders GABA hyperpolarizing during neuronal maturation. *Nature*, **397**, 251–255.

Romo-Parra, H., Trevino, M., Heinemann, U. & Gutierrez, R. (2008) GABA actions in hippocampal area CA3 during postnatal development: differential shift from depolarizing to hyperpolarizing in somatic and dendritic compartments. *J. Neurophysiol.*, **99**, 1523–1534.

Rovira, C. & Ben-Ari, Y. (1993) Developmental study of benzodiazepine effects on monosynaptic GABAA-mediated IPSP of rat hippocampal neurons. *J. Neurophysiol.*, **70**, 1076–1085.

Rudomin, P. & Schmidt, R.F. (1999) Presynaptic inhibition in the vertebrate spinal cord revisited. *Exp. Brain Res.*, **129**, 1–37.

Serafini, R., Valeyev, A.Y., Barker, J.L. & Poulter, M.O. (1995) Depolarizing GABA-activated Cl^- channels in embryonic rat spinal and olfactory bulb cells. *J. Physiol. (Lond.)*, **488**, 371–386.

Staley, K.J. & Mody, I. (1992) Shunting of excitatory input to dentate gyrus granule cells by a depolarizing GABAA receptor-mediated postsynaptic conductance. *J. Neurophysiol.*, **68**, 197–212.

Staley, K.J., Otis, T.S. & Mody, I. (1992) Membrane properties of dentate gyrus granule cells: comparaison of sharp microelectrode and whole-cell recordings. *J. Neurophysiol.*, **67**, 1346–1358.

Swann, J.W., Brady, R.J. & Martin, D.L. (1989) Postnatal development of GABA-mediated synaptic inhibition in rat hippocampus. *Neuroscience*, **28**, 551–561.

Szabadics, J., Varga, C., Molnar, G., Olah, S., Barzo, P. & Tamas, G. (2006) Excitatory effect of GABAergic axo-axonic cells in cortical microcircuits. *Science*, **311**, 233–235.

Tyzio, R., Ivanov, A., Bernard, C., Holmes, G.L., Ben Ari, Y. & Khazipov, R. (2003) Membrane potential of CA3 hippocampal pyramidal cells during postnatal development. *J. Neurophysiol.*, **90**, 2964–2972.

Tyzio, R., Cossart, R., Khalilov, I., Minlebaev, M., Hubner, C.A., Represa, A., Ben Ari, Y. & Khazipov, R. (2006) Maternal oxytocin triggers a transient inhibitory switch in GABA signaling in the fetal brain during delivery. *Science*, **314**, 1788–1792.

Tyzio, R., Holmes, G.L., Ben-Ari, Y. & Khazipov, R. (2007) Timing of the developmental switch in GABA(A) mediated signalling from excitation to inhibition in CA3 rat hippocampus using gramicidin perforated patch and extracellular recordings. *Epilepsia*, **48**, 96–105.

Verheugen, J.A., Fricker, D. & Miles, R. (1999) Noninvasive measurements of the membrane potential and GABAergic action in hippocampal interneurons. *J. Neurosci.*, **19**, 2546–2555.

Vida, I., Bartos, M. & Jonas, P. (2006) Shunting inhibition improves robustness of gamma oscillations in hippocampal interneuron networks by homogenizing firing rates. *Neuron*, **49**, 107–117.

Wang, D.D., Krueger, D.D. & Bordey, A. (2003) GABA depolarizes neuronal progenitors of the postnatal subventricular zone via GABAA receptor activation. *J. Physiol.*, **550**, 785–800.

Woodin, M.A., Ganguly, K. & Poo, M.M. (2003) Coincident pre- and postsynaptic activity modifies GABAergic synapses by postsynaptic changes in Cl-transporter activity. *Neuron*, **39**, 807–820.

Yamada, J., Okabe, A., Toyoda, H., Kilb, W., Luhmann, H.J. & Fukuda, A. (2004) Cl-uptake promoting depolarizing GABA actions in immature rat neocortical neurones is mediated by NKCC1. *J. Physiol.*, **557**, 829–841.

Zhang, S.J. & Jackson, M.B. (1993) GABA-activated chloride channels in secretory nerve endings. *Science*, **259**, 531–534.

Zhang, L., Spigelman, I. & Carlen, P.L. (1991) Development of GABA-mediated chloride-dependent inhibition in CA1 pyramidal neurones of immature rat hippocampal slices. *J. Physiol. (Lond.)*, **444**, 25–49.